



Boldine Attenuates Synaptic Failure and Mitochondrial Deregulation in Cellular Models of Alzheimer's Disease

Juan P. Toledo^{1†}, Eduardo J. Fernández-Pérez^{1†}, Ildete L. Ferreira^{2,3}, Daniela Marinho^{2,3}, Nicolas O. Riffo-Lepe¹, Benjamin N. Pineda-Cuevas¹, Luis F. Pinochet-Pino¹, Carlos F. Burgos¹, A. Cristina Rego^{2,4*} and Luis G. Aguayo^{1*}

¹ Laboratory of Neurophysiology, Department of Physiology, Universidad de Concepción, Barrio Universitario, Concepción, Chile, ² CNC-Center for Neuroscience and Cell Biology, University of Coimbra, Coimbra, Portugal, ³ IIIUC-Institute for Interdisciplinary Research, University of Coimbra, Coimbra, Portugal, ⁴ FMUC-Faculty of Medicine, University of Coimbra, Coimbra, Portugal

OPEN ACCESS

Edited by:

Philippe De Deurwaerdere,
Université de Bordeaux, France

Reviewed by:

Lucía Nuñez,
University of Valladolid, Spain
Wei Cui,
Ningbo University, China

*Correspondence:

A. Cristina Rego
acrego@cnc.uc.pt
Luis G. Aguayo
laguayo@udec.cl;
luisagua@gmail.com

†These authors have contributed
equally to this work

Specialty section:

This article was submitted to
Neuropharmacology,
a section of the journal
Frontiers in Neuroscience

Received: 27 October 2020

Accepted: 25 January 2021

Published: 19 February 2021

Citation:

Toledo JP, Fernández-Pérez EJ,
Ferreira IL, Marinho D, Riffo-Lepe NO,
Pineda-Cuevas BN, Pinochet-Pino LF,
Burgos CF, Rego AC and Aguayo LG
(2021) Boldine Attenuates Synaptic
Failure and Mitochondrial
Deregulation in Cellular Models
of Alzheimer's Disease.
Front. Neurosci. 15:617821.
doi: 10.3389/fnins.2021.617821

Alzheimer's disease (AD) is the most common cause of senile dementia worldwide, characterized by both cognitive and behavioral deficits. Amyloid beta peptide (A β) oligomers (A β O) have been found to be responsible for several pathological mechanisms during the development of AD, including altered cellular homeostasis and synaptic function, inevitably leading to cell death. Such A β O deleterious effects provide a way for identifying new molecules with potential anti-AD properties. Available treatments minimally improve AD symptoms and do not extensively target intracellular pathways affected by A β O. Naturally-derived compounds have been proposed as potential modifiers of A β -induced neurodysfunction and cytotoxicity based on their availability and chemical diversity. Thus, the aim of this study was to evaluate boldine, an alkaloid derived from the bark and leaves of the Chilean tree *Peumus boldus*, and its capacity to block some dysfunctional processes caused by A β O. We examined the protective effect of boldine (1–10 μ M) in primary hippocampal neurons and HT22 hippocampal-derived cell line treated with A β O (24–48 h). We found that boldine interacts with A β *in silico* affecting its aggregation and protecting hippocampal neurons from synaptic failure induced by A β O. Boldine also normalized changes in intracellular Ca²⁺ levels associated to mitochondria or endoplasmic reticulum in HT22 cells treated with A β O. In addition, boldine completely rescued the decrease in mitochondrial membrane potential ($\Delta\Psi$ m) and the increase in mitochondrial reactive oxygen species, and attenuated A β O-induced decrease in mitochondrial respiration in HT22 hippocampal cells. We conclude that boldine provides neuroprotection in AD models by both direct interactions with A β and by preventing oxidative stress and mitochondrial dysfunction. Additional studies are required to evaluate the effect of boldine on cognitive and behavioral deficits induced by A β *in vivo*.

Keywords: Alzheimer's disease, Boldine, mitochondria, synaptic transmission, intracellular Ca²⁺

INTRODUCTION

Alzheimer's Disease (AD) is the most prevalent neurodegenerative disorder characterized by cognitive and behavioral deficits (Terry et al., 1991) that is expected to reach 82 million cases in 2030 (Weidner and Barbarino, 2019). Age-related forms of dementia lead to sporadic AD. Conversely, less than 1% of cases are associated with familial forms due to mutations in the presenilin 1 or presenilin 2 genes involved in the processing of the amyloid precursor protein (APP) (Masters et al., 2015). AD pathology shows progressive neuronal damage and atrophy in vulnerable brain regions and circuits involved in memory, specifically in the hippocampus and cerebral cortex. These events appear to be preceded by synaptic and neuronal dysfunction. Neuropathologically, AD is characterized by the presence of extracellular plaques mainly composed of misfolded fibrillar amyloid beta peptide (A β) derived from the amyloidogenic processing of the APP by β - and γ -secretases, and intraneuronal neurofibrillary tangles consisting of aggregates of hyperphosphorylated tau protein (Ferreira et al., 2012b; Cline et al., 2018, for review). We previously reported that treatment (24 h) of hippocampal neurons with A β oligomers (A β O), but not monomers or fibers, reduced synaptic transmission evidenced by a large reduction in frequency of evoked and miniature currents, together with a number of presynaptic markers, that included SV2 (Parodi et al., 2010). In more recent studies, we have confirmed these original findings on the synaptotoxicity of A β O and further characterized the toxic components of these A β assemblies by oligomerization time curves, characterization of dimer and tetramers and by atomic force microscopy that reported nanometric structures (González-Sanmiguel et al., 2020).

Additionally, synaptic depression was associated with disruption of glutamatergic transmission that results from internalization of *N*-methyl-D-aspartate (NMDA) receptors (NMDARs) caused by A β O, ultimately leading to early cognitive deficits (Snyder et al., 2005; Cline et al., 2018, for review). Accordingly, it was previously demonstrated that A β O (1 μ M) pre-exposure reduces NMDA-evoked intracellular free Ca $^{2+}$ (Ca $^{2+}$ _i). Additionally, A β O *per se* induces an immediate Ca $^{2+}$ _i rise involving GluN2B-containing NMDARs in cortical neurons (Ferreira et al., 2012a).

On the other hand, mitochondria play a pivotal role in energy metabolism and neuronal Ca $^{2+}$ buffering in neurons. Indeed, mitochondria take up Ca $^{2+}$ in response to small increases in intracellular Ca $^{2+}$ _i levels (Naia et al., 2017, for review). In addition, mitochondria are in close physical contact with the endoplasmic reticulum (ER) in a structure formed by a myriad of proteins and several tethers named mitochondria-associated membranes (MAMs). This tight juxtaposition favors Ca $^{2+}$ exchange and signaling between the two organelles (Csordás et al., 2018). In our previous studies, we found that neuron exposure to A β O plus NMDA (mimicking imbalanced glutamatergic neurotransmission) potentiates the increase in Ca $^{2+}$ _i levels compared to A β O or NMDA alone (Ferreira et al., 2012a), leading to augmented mitochondrial Ca $^{2+}$ retention and mitochondrial depolarization through a pathway that involves ER IP3R and the mitochondrial Ca $^{2+}$ uniporter

(MCU) (Ferreira et al., 2015), highlighting the involvement of ER-mitochondria interplay in abnormal Ca $^{2+}$ homeostasis. In addition, A β O depletes ER-Ca $^{2+}$ through IP3R- and RyR-mediated Ca $^{2+}$ release increasing Ca $^{2+}$ _i levels and therefore compromising cell survival (Resende et al., 2008). In addition, generation of A β -induced ion channels cause aberrant cell excitability and accumulation of Ca $^{2+}$ _i (Snyder et al., 2005; Lei et al., 2016) causing an enhanced release of neurotransmitters and synaptic depletion (Sepúlveda et al., 2014). Ultimately, the sum of all of these conditions causes a loss of synaptic plasticity and cell death (Lambert et al., 1998; De Felice et al., 2008). Mitochondrial Ca $^{2+}$ overload induces disruption of mitochondrial respiration and ATP synthesis. Concomitantly, excessive production of reactive oxygen species (ROS) triggered by mitochondrial dysfunction and ER stress culminates in the oxidative damage observed in AD cells and animal models, as well as in AD patient's biological fluids and peripheral blood mononuclear cells (PBMCs) (Ferreira et al., 2012b; Mota et al., 2015).

Cholinesterase inhibitors and memantine (uncompetitive NMDAR antagonist) are the only drugs approved by the Food and Drug Administration (FDA) to slowdown the cognitive symptoms in the early and late stages of AD, respectively, however, neither of them inhibit the disease progression. Therefore, the development and testing of new drugs, such as natural compounds, is imperative as a primary prevention of cognitive decline associated with AD (Tewari et al., 2018; Cummings et al., 2019).

Boldine is an aporphinoid alkaloid derived from the wood and leaves of the Chilean tree *Peumus boldus* (commonly known as boldo) and traditionally consumed in South America (Cassels et al., 2018). Boldine structure is very similar to apomorphine, a molecule that was previously demonstrated to be neuroprotective in a 3xTg-AD mouse model by promoting the degradation of intraneuronal A β (Himeno et al., 2011). Boldine has been proposed to have potent antioxidant (Bannach et al., 1996), anti-inflammatory (Backhouse et al., 1994), anticonvulsive (Moezi et al., 2018), antihypertensive (Lau et al., 2013) and antidiabetic properties (Hernández-Salinas et al., 2013). In a previous study, a reduction in the inflammatory brain response was reported in glial cells in an APP^{swe}/PS1^{dE9} model of AD (Yi et al., 2017), although these investigators used much higher concentrations for *in vitro* experiments than those used in the present study.

Therefore, the aim of this study was to characterize the effects of boldine on A β O aggregation *in vitro* on A β O-induced synaptic impairment and postsynaptic currents in mature hippocampal neurons and on mitochondrial and ER-Ca $^{2+}$ retention, mitochondrial function, and ROS levels in a HT22 mouse hippocampal-derived cell line. Overall, our data with boldine shows that it attenuates A β -induced synaptic deficits and mitochondrial dysfunction in AD cell models.

MATERIALS AND METHODS

Reagents

Boldine was purchased from Sigma (Germany) and a 50 mM stock solution was prepared in DMSO and stored at -20°C according to manufacturer indications. Synthetic A β ₁₋₄₂

was purchased from Bachem (Bubendorf, Switzerland) and reconstituted following the instructions of the manufacturer. A β_{1-42} oligomers used in HT22 cells (referred as A β O) were prepared as previously described (Ferreira et al., 2012a). For electrophysiological studies, A β O were prepared as previously reported (Peters et al., 2013; González-Sanmiguel et al., 2020). For instance, A β_{1-42} was dissolved in hexafluoroisopropanol (HFIP, 10 mg/mL) and stored in aliquots at -20°C . For A β O preparation (80 μM), aliquots of 5 mL were added to 137.5 mL ultrapure water in an Eppendorf tube. After 15 min incubation at room temperature, the samples were centrifuged at 14,000 g for another 15 min, and the supernatant fraction transferred to a new tube. The samples were stirred at 500 rpm using a Teflon-coated microstir bar for 24–48 h at room temperature (approximately 22°C) and stored at 4°C until required. Fura2-AM and TMRM⁺ were purchased from Molecular Probes-Invitrogen (Eugene, OR, United States). Poly-L-lysine, MitoPY1, oligomycin, FCCP and 3-(4,5-dimethyl-2-thiazolyl)-2,5-diphenyl-2H-tetrazolium bromide (MTT) were purchased from Sigma Chemical Co. (St. Louis, MO, United States). Thapsigargin was purchased from Tocris Bioscience (Bristol, United Kingdom). The monoclonal mouse anti-synaptic vesicle protein 2 (SV2) antibody was from Developmental Studies (HybridomaBank, Iowa City, IA, United States) and rabbit anti-MAP2 was from Santa Cruz Biotechnology (Dallas, TX CA, United States). Anti-rabbit IgG conjugated with Cy5 and anti-mouse IgG conjugated with Cy3 were from Jackson Immuno Research Laboratories (West Grove, PA, United States). DAKO mounting medium was purchased from Agilent, United States. All other reagents were of analytical grade. The final concentration of DMSO in assays was not higher than 1% v/v.

Docking Simulations

In order to study the *in silico* interaction between boldine and A β_{1-42} , a protein-ligand docking was performed. First, the interaction grids (15 Å) for the C-terminal, central regions and full peptide were generated using the structure of monomeric A β_{1-42} (PDB ID: 1IYT) with Glide (Schrödinger, LLC, New York, NY). Boldine structure was obtained from PubChem (CID: 10154). A protein-ligand docking was performed using Glide with a high precision (XP) configuration. The complexes were analyzed using the docking score provided by Glide and the calculation of the MM-GBSA ΔG_{bind} using Prime (Schrödinger, LLC, New York, NY). All images presented were created with PyMOL (Schrödinger, LLC, New York, NY).

Aggregation Assay

For the aggregation and experiments in hippocampal neurons, we used a synthetic A β_{1-42} peptide obtained from Genemed Synthesis, Inc. (United States). Oligomeric species were prepared by measuring absorbance of A β samples at 23°C (Peters et al., 2020). We studied the inhibition of A β_{1-42} (40 μM) aggregation with GBP for 24 h under a stirring condition of 500 rpm. Absorbance at 405 nm was measured for 9 h with readings every 20 min using a Novostar microplate reader (BMG Labtech, United States). Protein absorbance was measured at 482 nm and all the experiments were performed in triplicates. Briefly, 40 μM

A β was added to a 96 well plate in the presence and absence of 10 and 100 μM boldine.

Primary Culture of Hippocampal Neurons

Hippocampal neurons were obtained from C57BL/J6 mice or Sprague-100 Dawley rat embryos as previously described (e.g., Aguayo and Pancetti, 1994). Animal care and protocols were in accordance with the National Institutes of Health (NIH) recommendations and approved by the Ethics Committee at the University of Concepcion. Briefly, hippocampal tissue was harvested from 18 to 19 days old embryos. The pregnant animal was anesthetized with CO_2 and subsequently euthanized by cervical dislocation. The embryos were removed and rapidly decapitated. Brains were removed and the hippocampi were dissected from the cortices free of meninges. The hippocampus was mechanically and enzymatically dissociated (Aguayo and Pancetti, 1994). After being isolated, neurons were plated at 250,000 cells/mL on coverslips precoated with poly-L-lysine in 90% minimal essential medium (MEM; Gibco, Grand Island, NY, United States), 5% heat-inactivated horse serum (Gibco), 5% fetal bovine serum (Gibco) and supplemented with N3 (mg/mL: BSA 1, putrescine 3.2, insulin 1, apotransferrin 5, corticosterone 0.5 (g/mL: sodium selenite 5, TH3 0.5, progesterone 0.6). Cultures were maintained in a humidified atmosphere at 37°C containing 95% air and 5% CO_2 for 8–10 days. Culture medium was partially replaced every 3 days. Hippocampal neurons (10 DIV) were treated with 1 μM A β O in the presence or absence of 10 μM boldine for 24 h.

Electrophysiological Recordings

For voltage-clamp experiments in the whole cell mode, culture medium was replaced with a normal external solution (NES) containing: 150 mM NaCl, 5.4 mM KCl, 2 mM CaCl_2 , 1 mM MgCl_2 , 10 mM glucose and 10 mM HEPES, pH 7.4/NaOH; 320 mOsm/L). Cells were stabilized at room temperature for 20 min before experiments. The internal solution used to record spontaneous post-synaptic currents (sPSCs) contained 120 mM KCl, 2.0 mM MgCl_2 , 2 mM Na_2ATP , 10 mM BAPTA, 0.5 mM NaGTP and 10 mM HEPES, pH 7.4/KOH; 310 mOsm/L). All currents were recorded by adjusting the membrane potential to -60 mV using an Axopatch-200B amplifier (Molecular Devices, United States) and an inverted microscope (Nikon Eclipse TE200-U, Japan). The acquisition was made using a computer connected to the recording system with a Digidata 1440A acquisition card (Molecular Devices, United States) and the pClamp10 software (Molecular Devices, United States). Electrodes with a resistance of 4–5 M Ω were pulled from borosilicate capillaries (WPI, United States) in a horizontal puller (P1000, Sutter Instruments, United States). A 5 mV pulse was used to monitor series resistance throughout the recording period and only cells with a stable access resistance (less than 15 M Ω and that did not change more than 20%) were included for data analysis. After acquiring the synaptic recording, the area under the current trace was integrated (pA·ms) and expressed as charge transferred (nC) during the whole recording period (2 min) using Clampfit 10.5 (Molecular Devices, United States).

Immunocytochemistry

Hippocampal neurons were fixed for 15 min with 4% paraformaldehyde in PBS. Thereafter, cells were incubated with permeabilization and blocking solution with 0.1% Triton X-100 in horse serum (HS):PBS 1:10 for 20 min. Cells were then incubated with primary antibodies [monoclonal mouse anti-synaptic vesicle 2 protein (SV2) antibody (1:200) and rabbit anti-MAP2 (1:300)] overnight at 4°C followed by incubation with secondary antibodies [anti-rabbit IgG conjugated with Cy5 (1:500) and anti-mouse IgG conjugated with Cy3 (1:500)] for 2 h at room temperature. All antibodies were diluted with HS (10%) in PBS. Coverslips were mounted in DAKO mounting medium and cells observed under a spectral confocal laser scanning microscope (LSM780, Zeiss, Germany) using a 63 × 1.4 numerical aperture oil immersion objective (Zeiss, Germany). Images of 16-bit were collected using a pixel time of 1.58 μs and a pixel size of 110 nm.

Quantification of SV2 Fluorescent Puncta

In fluorescence microscopy, light undergoes diffraction while traveling in an imaging system leading to image blurring and limiting visual access to details. The blurring is characterized by a point-spread function (PSF) that along with the original image can be used in a deconvolution algorithm to restore microscopic details. Therefore, using the Richardson–Lucy algorithm provided by DeconvolutionLab2 plugin (Sage et al., 2017) in Image J (NIH) and a theoretical PSF (based on imaging parameters), we deconvolved and analyzed the confocal micrographs of neurons that were immunostained for synaptic vesicle 2 (SV2), a presynaptic marker. Deconvolution was followed by maximum intensity z-projection and background adjustment. Using the MAP-2 signal, we generated a mask to only obtain the signal of SV2 in the neuron where the analysis was carried out. The micrographs were used to quantify the size and number of fluorescent punctas of SV2 (or clusters) on the first 20 μm of neuronal primary processes using measuring tools from Image J software. At least 30 processes *per* condition were counted.

HT22 Cell Culture and Treatment

HT22 cells, a mouse hippocampal cell line obtained from the immortalization of primary hippocampal neurons using a temperature sensitive SV40 T-antigen and subcloned from HT4 cells based on sensitivity to glutamate (Davis and Maher, 1994), were obtained from Dr. Dave Schubert (Salk Institute, La Jolla). The cells were grown in 75 cm² culture flasks in high-glucose Dulbecco's Modified Eagle's medium (DMEM) supplemented with 10% heat inactivated (HI) fetal bovine serum (FBS), 12 mM NaHCO₃, 5 mM HEPES and 100 μg/mL penicillin-streptomycin, pH 7.3 in a humidified incubator with 5% CO₂ and 95% air at 37°C. When 80% confluency was reached, cells were detached using a Ca²⁺-Mg²⁺-free dissociation medium containing 140 mM NaCl, 8.1 mM Na₂HPO₄, 1.47 mM KH₂PO₄, 1.47 mM KCl, 0.55 mM EDTA, pH 7.3 and then centrifuged at 800 rpm for 5 min and subsequently sub-cultured or plated at a density of 0.005 × 10⁶ cell/well in 96-multiwell plates.

Twenty four hour after plating, cells were treated with 1 μM AβO in the presence or absence of 1, 10 or 100 μM boldine in culture conditioned medium (medium where the cells were plated) for 24 h at 37°C in a humidified culture chamber containing 95% O₂ and 5% CO₂. The effect of boldine alone was also tested.

MTT Assay

Cell viability was determined using the colorimetric MTT assay based on the reduction of MTT into an insoluble formazan product via nicotinamide adenine dinucleotide phosphate (NADH)-dependent dehydrogenases by viable cells. HT22 cells were incubated with 0.5 g/L MTT in Krebs medium containing 135 mM NaCl, 5 mM KCl, 1.8 mM CaCl₂, 0.4 mM KH₂PO₄, 1 mM MgSO₄, 5.5 mM glucose, 20 mM HEPES, pH 7.4 for 2 h at 37°C in the dark. Krebs medium was removed and formazan crystals were dissolved in 0.04 M HCl in isopropanol. The absorbance at 570 nm was then measured spectrophotometrically using a SpectraMax plus microplate reader (Molecular Devices, United States).

Mitochondrial and ER-Ca²⁺ and ΔΨ_m Measurement

For mitochondrial-Ca²⁺ and ΔΨ_m measurements, HT22 cells were rinsed with Krebs medium and co-loaded with the high affinity Ca²⁺ probe Fura2-AM (5 μM) that accumulates in the cytoplasm plus the ΔΨ_m sensing dye TMRM⁺ (300 nM; under quenched mode) that accumulates in polarized mitochondria, for 40 min at 37°C. Cells were then rinsed with Krebs medium and fluorescence was measured in the presence of TMRM⁺ (in order to prevent leakage) using a Spectrofluorometer Gemini EM (Molecular Devices, United States). The fluorescence was recorded for both Fura2 at 340/380 nm excitation and 510 emission, and for TMRM⁺ at 540 nm excitation and 590 nm emission. After the establishment of a 2-min baseline, cells were stimulated with 2 μM FCCP to induce maximal mitochondrial depolarization in the presence of 2 μg/mL oligomycin, to prevent ATP hydrolysis. The cytoplasmic Ca²⁺ increase upon mitochondrial Ca²⁺ release was recorded as an increase in the Fura2 fluorescence, whereas ΔΨ_m was evaluated by the increase in TMRM⁺ fluorescence signal in response to mitochondrial full depolarization. For ER-Ca²⁺ measurements, cells were incubated in Fura2-containing Krebs medium for 30 min at 37°C. Following a washing step, fluorescence was measured in Ca²⁺-free Krebs medium. After the baseline establishment, cells were stimulated with 1 μM thapsigargin, a selective non-competitive inhibitor of sarcoendoplasmic reticulum Ca²⁺-ATPase (SERCA), that leads to ER-Ca²⁺ depletion. The increase in Fura2 fluorescence signal was recorded and analyzed as relative levels of ER-Ca²⁺. Fluorescence was measured using a Spectrofluorometer Gemini EM (Molecular Devices, United States). Ca²⁺ levels and ΔΨ_m presented in bar graphs were calculated by subtracting the last baseline value (before stimuli) to the highest fluorescence value after the stimuli.

Mitochondrial H₂O₂ Analysis

HT22 cells were rinsed with Krebs medium and loaded with 10 μ M mitochondrial peroxy yellow 1 (MitoPY1), a fluorescent probe that selectively accumulates in the mitochondria and reacts with H₂O₂. Cells were incubated with the probe during 20 min at 37°C in a humidified culture chamber containing 95% O₂ and 5% CO₂. Then, cells were rinsed with Krebs medium and fluorescence was read at 489 excitation and 540 emission in a Spectrofluorometer Gemini EM (Molecular Devices, United States).

Analysis of Mitochondrial Oxygen Consumption Rate by Seahorse Analyzer

O₂ consumption by HT22 cells, cultured as described before, was measured by using the XF24 flux analyzer according to Ferreira et al. (2018). HT22 cells were plated on XF24 microplates at a density of 0.3×10^4 cells per well 48 h before the experiments. On the following day, cells were incubated with or without 1 μ M A β O in the absence or in the presence of 1 μ M boldine and cultured for an additional 24 h. The effect of boldine alone was also tested. On the day of experiments, cell culture medium was carefully removed and cells were washed two times with 1 mL DMEM5030 medium, pH 7.4, supplemented with 2 g/L glucose and 0.3 g/L glutamine to fully remove the previous medium. Then, the cells were incubated in 450 μ L DMEM at 37°C in a CO₂-free incubator for 1 h. Cellular bioenergetics was determined using the extracellular flux analyzer (Seahorse Bioscience). This system allows for real time, non-invasive measurements of oxygen consumption rate (OCR), which can be correlated with mitochondrial function/oxidative burst. Sequential injection of mitochondrial inhibitors oligomycin (2.5 μ g/mL), FCCP (4 μ M), and antimycin A (AntA; 4 μ M) plus rotenone (2 μ M) were added to evaluate basal respiratory capacity, maximal respiration in the presence of FCCP, oligomycin-sensitive O₂ consumption coupled to ATP synthesis, proton leak, spare respiratory capacity and non-mitochondrial respiration as previously described (Ferreira et al., 2018). Results are expressed in picomoles of O₂ per minute (pmol O₂/min).

Statistical Analysis

Data were analyzed by using Excel and GraphPad Prism 8 (GraphPad Software, San Diego, CA, United States) software and results are expressed as the mean \pm SEM. Comparison among groups was performed using the Kruskal-Wallis test followed by uncorrected Dunn's multiple comparisons test or one-way ANOVA followed by Tukey's *post hoc* test. Statistical differences were represented as * p < 0.05, ** p < 0.01, *** p < 0.001.

RESULTS

Boldine Interacts With A β _{1–42} *in silico*

The C-terminal region of the A β peptide was found to play an important role in its aggregation, membrane association, pore formation and toxicity of the A β peptide (Peters et al., 2013).

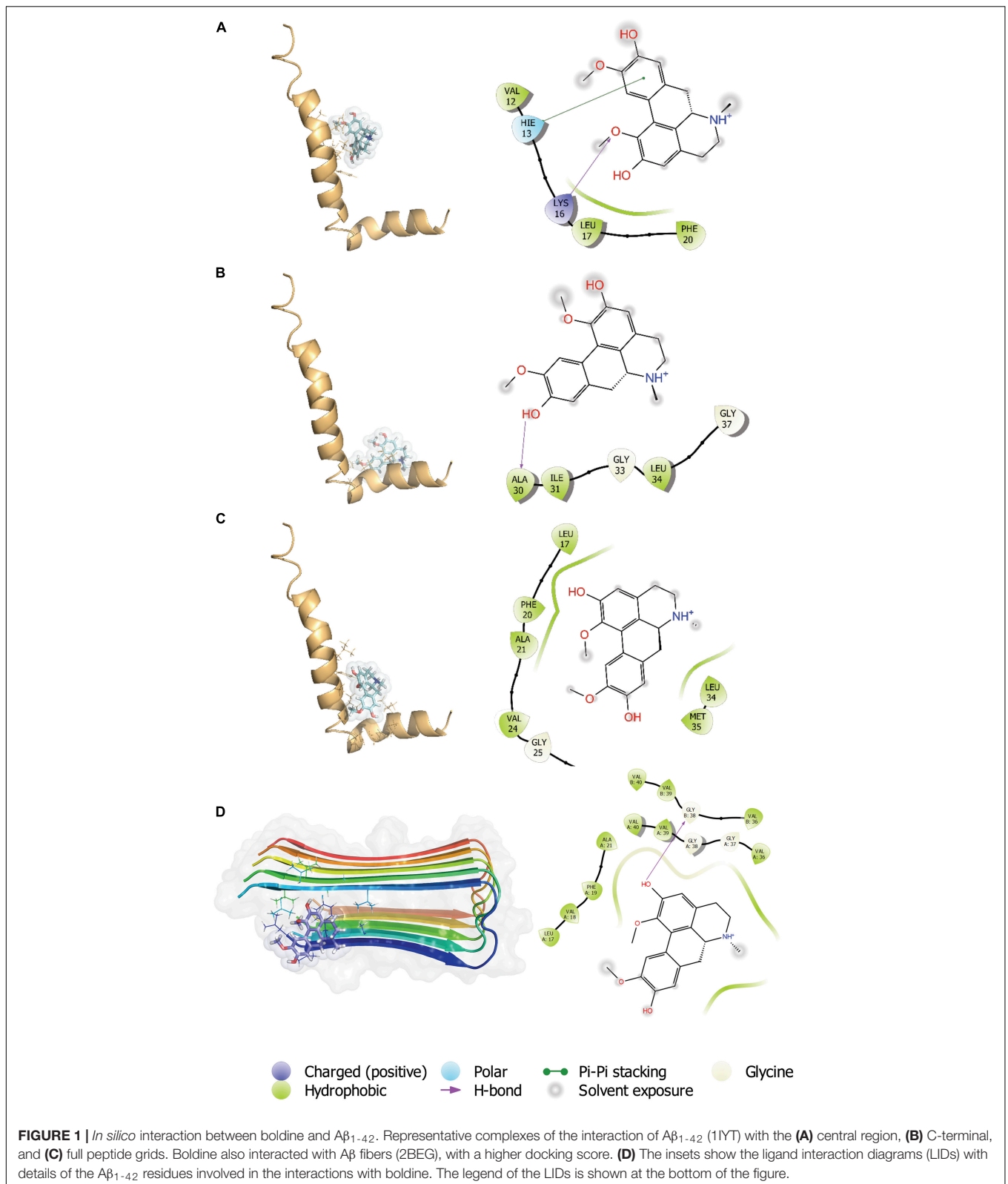
During a massive screening of small molecules with capacity to interact with the C-terminal region (Peters et al., 2020), we found several molecules having a high docking score and ΔG_{bind} (MM-GBSA), one of which was boldine (Figure 1A). Therefore, additional assessment of boldine and A β _{1–42} peptide (1IYT) docking interactions was performed considering 3 grids: central region (Figure 1B), C-terminal (Figure 1C) regions and full peptide (Figure 1D). For the interaction between boldine and the central region of A β (Figure 1B), a docking score of -2.047 was obtained. Here, boldine interacted with residues VAL 12, HIS 13, LYS 16, LEU 17, and PHE 20. A Pi-Pi stacking interaction was established with HIS 13 and a hydrogen bridge with LYS 16. For interaction of boldine and the C-terminal region (Figure 1C), a docking score of -1.427 was obtained and the data shows that boldine interacted with ALA 30, ILE 31, GLY 33, LEU 34, and GLY 37, establishing hydrogen bridges with ALA 30. For the interaction with the full structure (Figure 1D), a docking score of -3.373 was obtained and we found that boldine interacted with several residues, namely ALA 17, PHE 20, ALA 21, VAL 24, GLY 25, LYS 28, LEU 34, MET 35. Boldine also interacted with A β fibers (2BEG), with the higher score of -4.596 . The residues found to interact with boldine were LEU 17, VAL 18, PHE 19, ALA 21, VAL 36 (x2), GLY 37, GLY 38 (2), VAL 39 (x2), and VAL 40 (x2). Therefore, boldine appears to affect several A β toxic species.

Boldine Reduces A β Aggregation

Since we found that boldine was able to interact with A β , we further examined if this interaction was due to inhibition of peptide aggregation. Therefore, we assessed the aggregation of A β (40 μ M) in the presence of two concentrations of boldine (10 and 100 μ M) under constant agitation. Results in Figure 2A demonstrate that A β aggregation levels reached a plateau at about 4 h, that is similar to our recent study that reported the presence of A β O tetramers and nanometric structures using AFM (González-Sanmiguel et al., 2020). The levels of A β aggregation, as reflected by a reduction in turbidimetry, were measured up to 9 h of incubation and compared with boldine alone (incubated in the same conditions) (Figure 2A). Our results show that boldine inhibited A β aggregation in a concentration-dependent manner (p < 0.05 and p < 0.01 for 10 and 100 μ M boldine, respectively) (Figure 2B). No signal was obtained in the presence of 100 μ M boldine alone.

Boldine Prevents Synaptic Impairment Induced by A β

To investigate if boldine was able to exert a protective action on the A β O induced synaptic impairment, similar to previous studies (Parodi et al., 2010; González-Sanmiguel et al., 2020; Peters et al., 2020), hippocampal neurons were treated for 48 h with 1 μ M A β O in the presence of 10 μ M boldine and further analyzed for SV2-labeled presynaptic vesicles by immunocytochemistry using confocal microscopy (Figure 3A). Quantification of SV2 puncta/20 μ m process length showed a significant reduction in SV2 labeling in A β O-treated neurons (p < 0.05) and this effect was reduced



when the neurons were co-incubated with A β O and 10 μ M boldine ($p < 0.05$) (Figure 3B), suggesting a protective effect of boldine against A β O-induced synaptic damage.

Moreover, incubation of the hippocampal neurons with 10 μ M boldine alone had no effect on the SV2 puncta (Figures 3A,B).

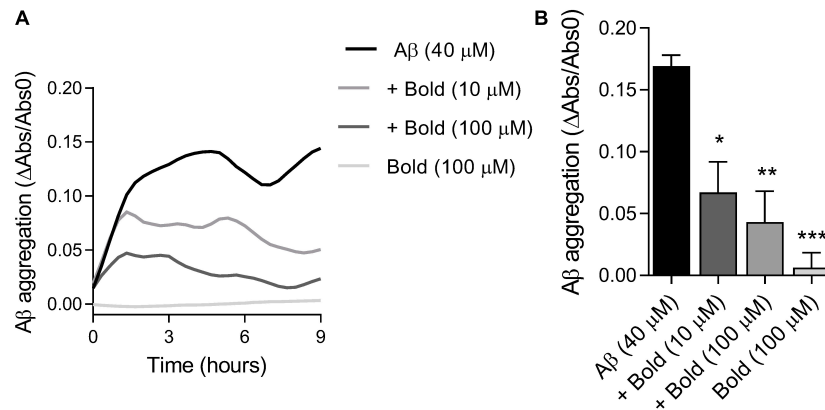


FIGURE 2 | Effect of boldine on A β aggregation *in vitro*. **(A)** Representative traces of A β (40 μ M) aggregation in the absence and presence of boldine (Bold; 10 or 100 μ M) or boldine alone (100 μ M). **(B)** A β aggregation levels after 9 h incubation (22–24°C) presented as the mean SEM of six replicates. Statistical analysis: One-way ANOVA followed by Tukey's multiple comparison test; * $p < 0.05$, ** $p < 0.01$, *** $p < 0.001$ when compared to A β .

To independently confirm the effect of boldine in recovering the SV2 protein labeling, and functionally preventing synaptic impairment, spontaneous synaptic currents were recorded at a holding potential (V_h) of -60 mV in neurons treated with A β O in the absence or presence of boldine using the whole-cell technique. Under voltage clamp conditions, bursts of synaptic activity were recorded reflected by synaptic events (Figure 4A, blue arrows) and faster spikes (red arrows) (Figure 4A). All these events were integrated as charge transferred and quantified (Figure 4B). The data showed that, compared with the control conditions, 1 μ M A β O caused a large reduction ($p < 0.01$) in the number and amplitude of the synaptic currents. Co-incubation of A β O with 10 μ M boldine significantly recovered the presence of postsynaptic currents and synaptic transmission. Boldine alone had no effect on the functional activity.

Boldine Prevents A β O-Induced Mitochondrial and ER-Ca $^{2+}$ Accumulation

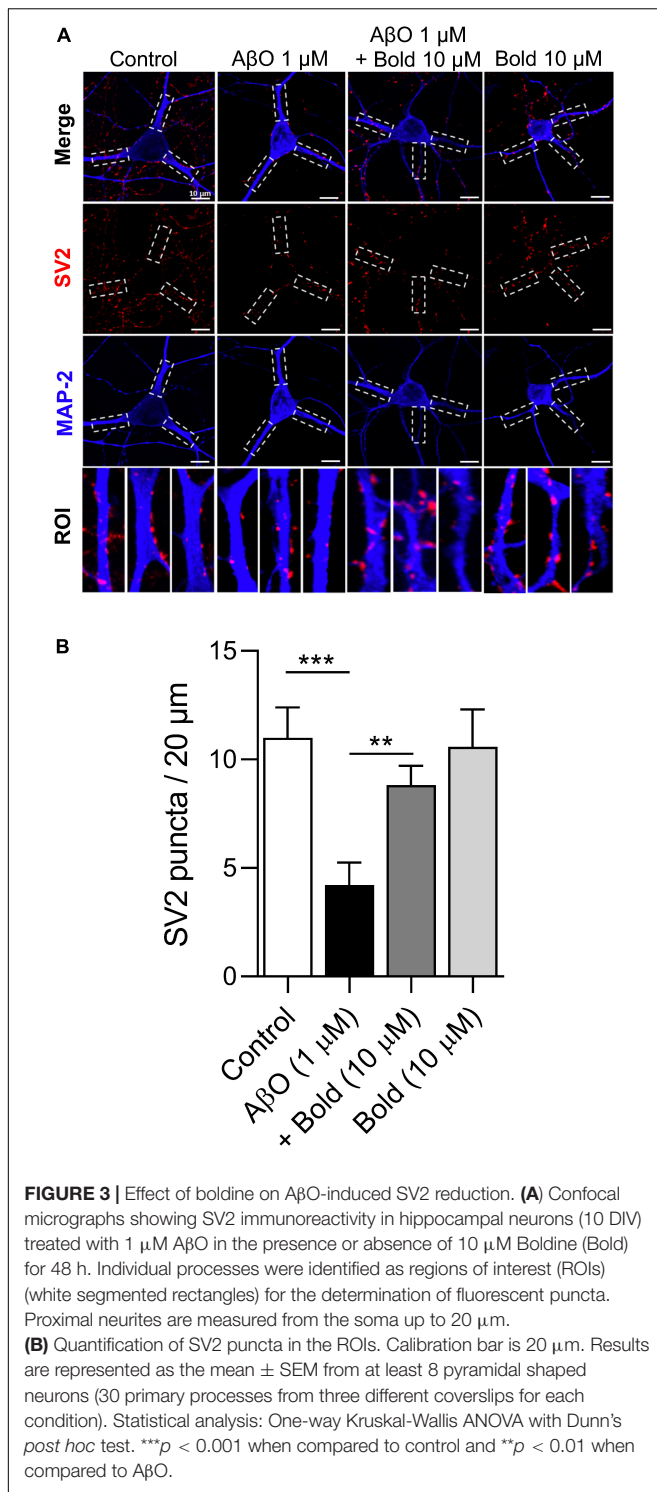
A β O-induced mitochondrial and ER-Ca $^{2+}$ overload plays a critical role on mitochondrial function, and consequently on bioenergetics and synaptic function (Reddy and Beal, 2008). Our results show that A β O-treated HT22 hippocampal-derived cells exhibited a significant increase in mitochondrial Ca $^{2+}$ levels ($p < 0.001$), as evidenced by the increase in cytosolic Ca $^{2+}$ rise following complete mitochondrial depolarization (with FCCP plus oligomycin) (Figure 5Ai). Moreover, A β O exposure enhanced ER-Ca $^{2+}$ levels ($p < 0.05$) as observed after ER-Ca $^{2+}$ depletion induced by 1 μ M thapsigargin (selective SERCA inhibitor) in HT22 cells (Figure 5B). Boldine completely abolished the augmented mitochondrial and ER-Ca $^{2+}$ retention induced by A β O ($p < 0.001$ and $p < 0.01$ for mitochondrial and ER-Ca $^{2+}$, respectively) (Figures 5Ai,B). Nevertheless, boldine itself had no effect on Ca $^{2+}$ accumulation in either organelle (Figures 5Ai,B). These results suggest that boldine is able to alleviate Ca $^{2+}$ -mediated ER and mitochondrial dysfunction caused by A β O.

Boldine Interferes With A β O-Mediated Changes in Mitochondrial Function and ROS Levels, Alleviating Cell Viability

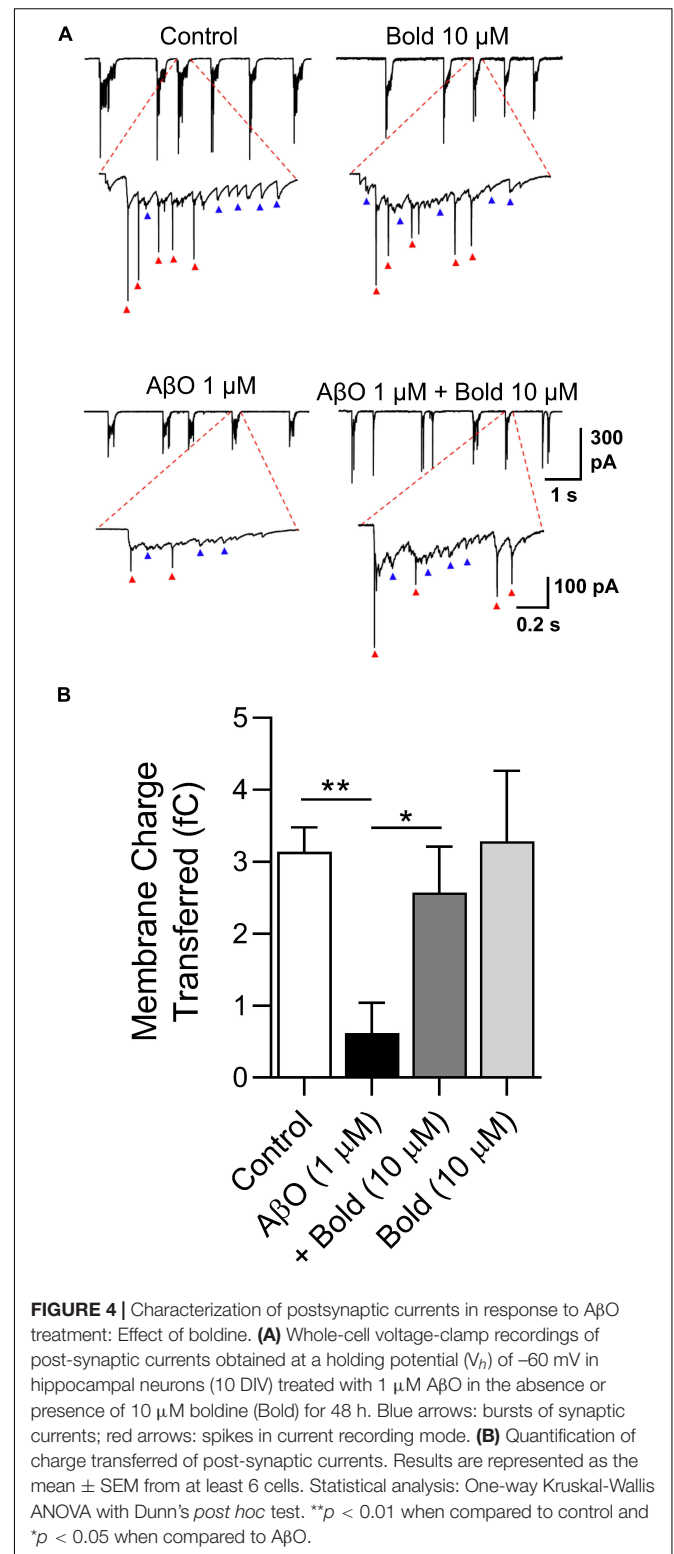
To further assess the role of boldine on mitochondrial function, $\Delta\Psi_m$ was assessed using TMRM $^+$, a fluorescent probe that predominantly accumulates in polarized mitochondria. Our results showed that A β O-treated HT22 cells exhibited a significant decrease in $\Delta\Psi_m$ ($p < 0.05$), which was largely prevented by 1 μ M boldine ($p < 0.001$) (Figure 5Aii). Treatment with boldine alone did not exert any effect on $\Delta\Psi_m$ (Figure 5Aii). These data highly suggest that compromised mitochondrial function in A β O-treated HT22 cells can be restored by boldine.

Based on these changes, we also examined mitochondrial ROS in HT22 cells labeled with MitoPY1, a probe that selectively reacts with H $_2$ O $_2$ produced by mitochondria. Our results indicate that A β enhanced mitochondrial ROS levels ($p < 0.05$) and this effect was largely prevented by co-treatment with boldine ($p < 0.001$) (Figure 5C). Boldine had no effect on mitochondrial ROS production in control cells (Figure 5C). HT22 neural cells incubated with 1 μ M A β O for 24 h also showed a decrease in cell viability as evaluated by the MTT assay. According with the previous results, boldine (1–10 μ M) had a neuroprotective role in this AD cell model ($p < 0.05$) (Figure 5D). Data shows that even at a high concentration (100 μ M) boldine does not affect cell viability (Figure 5D).

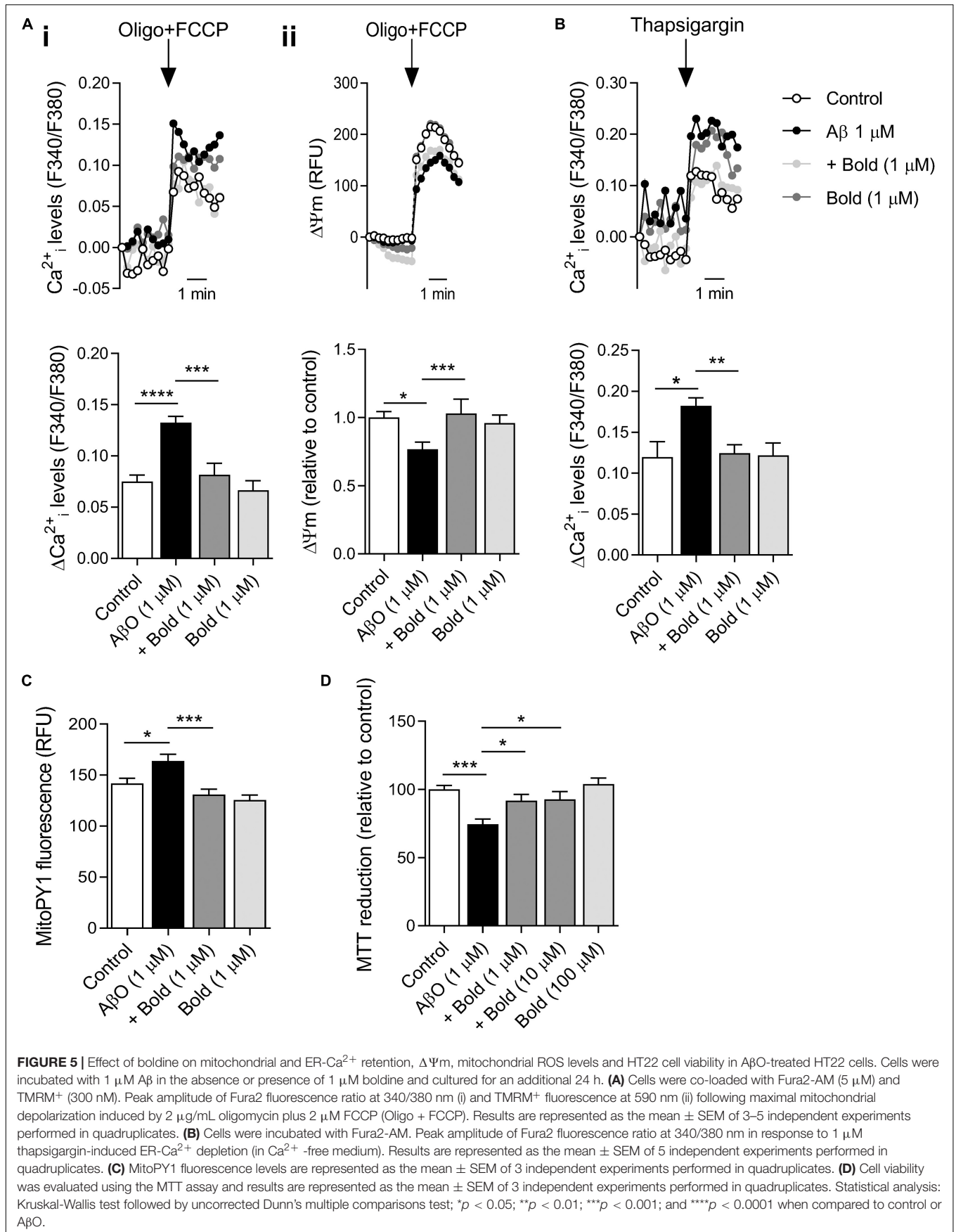
Because regulation of mitochondrial Ca $^{2+}$ levels is relevant for mitochondrial overall activity, we analyzed mitochondrial respiration profile and ATP synthesis in cells exposed to A β O and/or boldine. Mitochondrial respiration was analyzed in HT22 cells incubated with A β O in the absence or presence of boldine (1 μ M) by using a Seahorse XF24 flux analyzer (Figure 6) in which basal respiratory capacity, maximal respiration (in the presence of FCCP), oligomycin-sensitive oxygen consumption coupled to ATP synthesis, H $^+$ leak, spare respiratory capacity and non-mitochondrial respiration were measured (Figures 6A,B). Our results clearly demonstrated



significant decreases in maximal respiration, ATP synthesis, H⁺ leak and spare respiratory capacity in A β O-treated HT22 cells, while in the presence of A β O plus boldine oxygen consumption rates were similar to control conditions when assessing maximal respiration, H⁺ leak and spare respiratory capacity (Figures 6A,B). A β O or boldine induced no significant



changes in basal respiration, but boldine *per se* enhanced non-mitochondrial respiration (Figures 6A,B). No changes in glycolytic activity were detected under these conditions (data not shown).



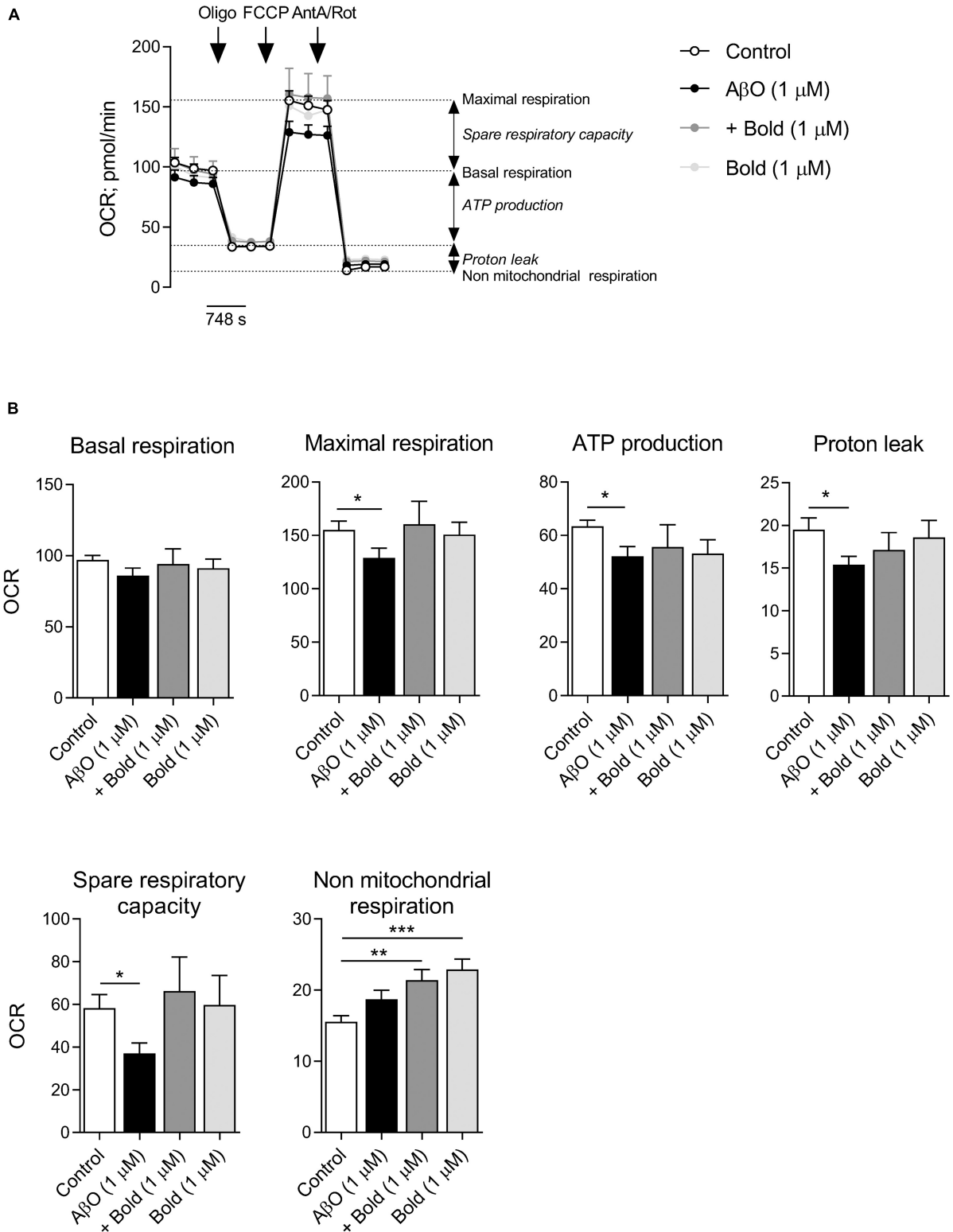


FIGURE 6 | Effect of boldine on oxygen consumption rate (OCR) in AβO-treated HT22 cells. Cells were incubated with 1 μM Aβ in the absence or presence of 1 μM boldine and cultured for an additional 24 h. **(A)** Traces of mitochondrial respiration before and after oligomycin (oligo), FCCP and antimycin A (AntA) plus rotenone (Rot) injection in cells treated with 1 μM Aβ and 1 μM boldine for 24 h. **(B)** Basal and maximal respiration, ATP production, proton leak, spare respiratory capacity and non-mitochondrial respiration. Results are presented as the mean ± SEM of 3–5 independent experiments performed in duplicates. Statistical analysis: Kruskal-Wallis test followed by uncorrected Dunn's multiple comparisons test; **p* < 0.05; ***p* < 0.01; and ****p* < 0.001 when compared to control.

These data demonstrate that cytoprotective effects of boldine in cells exposed to A β O largely involve its capacity to ameliorate mitochondrial function and redox profile.

DISCUSSION

The present study shows that boldine can interact with A β *in silico* and inhibit its aggregation at low micromolar concentrations. Boldine was also able to attenuate the synaptic failure induced by A β O, along with calcium and mitochondrial dyshomeostasis, suggesting that it could act as a natural anti-AD compound.

The analysis of *in silico* docking between boldine and A β provided an initial evidence supporting their association. This positive identification resulted from performing a much larger screening, looking for small molecules that could interact with the C-terminal region of A β . Previously, using FRET, aggregation assays and other techniques, we found that a small pentapeptide having the sequence of A β was able to associate and effectively block its synaptic toxicity (Peters et al., 2013). More recent studies using *in silico* docking, molecular dynamics, and *in vitro* and *in vivo* approaches allowed us to identify a small molecule with similar protective actions on the peptide (Peters et al., 2020). The present docking study expands on these previous results and shows that boldine, a Chilean tree-derived natural compound, interacts with several amino acids along the A β sequence such as glycine 33 and 37, previously shown to be important for the A β association to artificial lipid bilayers (Lin et al., 2008) and self-aggregation, in agreement with the idea that boldine can interfere with the formation of higher order complex species like oligomers and fibrils. We also showed that boldine interacted with glycine 25, which belongs to a motif of 14 residues (i.e., GLY25-GLY37) important for its aggregating properties (Jarrett and Lansbury, 1993; Peters et al., 2013). Boldine also interacts with histidines 13 and 14, recognized to be important for the permeation of ions through the amyloid channel (Nakamura et al., 2007). Thus, the data provide *in silico* evidence for an interaction between A β monomers and boldine. Interestingly, Arispe (2004) and Arispe et al. (2008) previously reported that small molecules that form complexes with these histidines blocked both the channel opening and its cytotoxicity. Consistent with an interaction between A β and boldine, the alkaloid was effective inhibiting the aggregation of A β *in vitro*. Interestingly, apomorphine, another structurally related aporphinoid, also showed anti-aggregation properties suggested to be related to structural changes of the peptide when interacting with apomorphine (Hanaki et al., 2018). As an anti-aggregation agent, apomorphine was able to inhibit the formation of amyloid plaques in the brain of 3xTg-AD mice (Himeno et al., 2011). At this moment, however, we do not have additional information on particular A β species that are more affected by boldine. It is interesting to note that apomorphine and boldine are aporphine alkaloids, thus they share a number of chemical and biological properties. In this way, and similar to apomorphine, boldine inhibited A β aggregation at very similar concentrations. A recent study using nuclear magnetic resonance showed that apomorphine interacted with Arg5, His13,14, Gln15,

and Lys16 of the A β ₁₋₄₂ monomer (Hanaki et al., 2018). Interestingly, our results show that several of these residues also participate in boldine interactions. Finally, the present *in silico* analysis also show that A β fibers can interact with boldine, suggesting that it can actually affect several species. Therefore, the inhibitory capacity of boldine on A β aggregation can be attributed to its interaction with the C-terminal region of the peptide, potentially interfering with the interaction of the peptide with the cellular membrane (Kim and Hecht, 2006; Lin et al., 2008). Interestingly, the study of macroscopic amyloid burden in 2xTgAD mice was not modified by long-term treatment with boldine added to drinking water (Yi et al., 2017). This negative result could be explained because the experiment involved a somewhat late stage of plaque formation (6 months) and because addition of boldine to drinking water does not guarantee brain delivery at therapeutic concentrations.

The synaptotoxicity produced by A β O is likely initiated by its capacity to alter membrane permeability causing a large, unregulated increase in intracellular Ca²⁺ levels through a cation-conducting pore at the plasma membrane. This leads to an early enhancement in neurotransmission that is followed by synaptic vesicle depletion and a loss of intercellular communication (Sepúlveda et al., 2014). The synaptotoxicity of A β O may be also related to the alteration of excitatory ligand-gated ion channels, such as the NMDARs and/or functional alterations of intracellular ion stores (e.g., ER, mitochondria), promoting Ca²⁺ dyshomeostasis (Shankar et al., 2007; Ferreira et al., 2012b). Results obtained by analyzing SV2-labeled presynaptic puncta, a good presynaptic marker (Parodi et al., 2010), indicated that boldine protects against A β O-induced synaptic impairment. The recovery in the presynaptic marker with boldine was in agreement with the increase in functional synaptic transmission found in A β O treated neurons. In previous studies, also supporting beneficial synaptic effects of boldine, it was found that a dose range of 3–25 mg/kg boldine administered to scopolamine-treated mice improved memory function (Dhingra and Soni, 2018) and ameliorated brain damage and cognitive deficits after cerebral artery occlusion (De Lima et al., 2016).

By altering A β aggregation, boldine can prevent A β O-induced Ca²⁺ accumulation in the cytosol. As such, A β O-induced Ca²⁺ accumulation in ER and mitochondria was alleviated following boldine treatment, and mitochondrial function was improved. ER and mitochondria contact sites establish microdomains for inter-organellar Ca²⁺ signaling at MAMs, which contain, efficient Ca²⁺-transport systems. Thus, boldine interfered with A β O-mediated direct or indirect mitochondrial effects linked to ATP production (e.g., complex IV) and oxidative stress (Rhein et al., 2009; Beck et al., 2016). In this respect, boldine alleviated the reduction in maximal respiration and largely increased spare respiratory capacity in cells treated with A β O, thus potentially enhancing ATP generation by oxidative phosphorylation in case of a sudden increase in energy demand.

Concordantly with changes in respiratory reserve, boldine interfered with A β O-mediated changes in $\Delta\Psi_m$ and ROS levels. Previously, treatment with boldine (10–20 mg/kg) was shown to restore $\Delta\Psi_m$ and ROS levels in a murine model of renal

dysfunction (Heidari et al., 2019). In addition, boldine restored $\Delta\Psi_m$ in high dopamine stressed PC12 cells (Youn et al., 2002). Under A β O conditions, voltage-dependent anion channel protein (VDAC) is overexpressed and aggregated inducing a decrease in $\Delta\Psi_m$ (Smilansky et al., 2015). Indeed, small molecules can inhibit VDAC aggregation, positively regulating $\Delta\Psi_m$ and energy imbalance caused by A β (Ben-Hail et al., 2016). Acting as a small molecule in A β O-treated hippocampal cells, boldine may have a similar effect to restore $\Delta\Psi_m$. Therefore, control of mitochondrial Ca^{2+} signals critically

regulate mitochondrial activity and maintain the $\Delta\Psi_m$, thereby affecting cell metabolism and survival.

In addition, boldine prevented mitochondrial H_2O_2 levels induced by A β O, which is in agreement with previous studies in several models indicating that the neuroprotective effects of boldine are due to its antioxidant effects (Konrath et al., 2008; De Lima et al., 2016). Boldine (50 mg/kg) inhibited ROS production and lipid peroxidation in hypertensive and diabetic rats (Jang et al., 2000; Hernández-Salinas et al., 2013; De Lima et al., 2016; Gómez and Velarde, 2018). In addition, Youn et al. (2002)

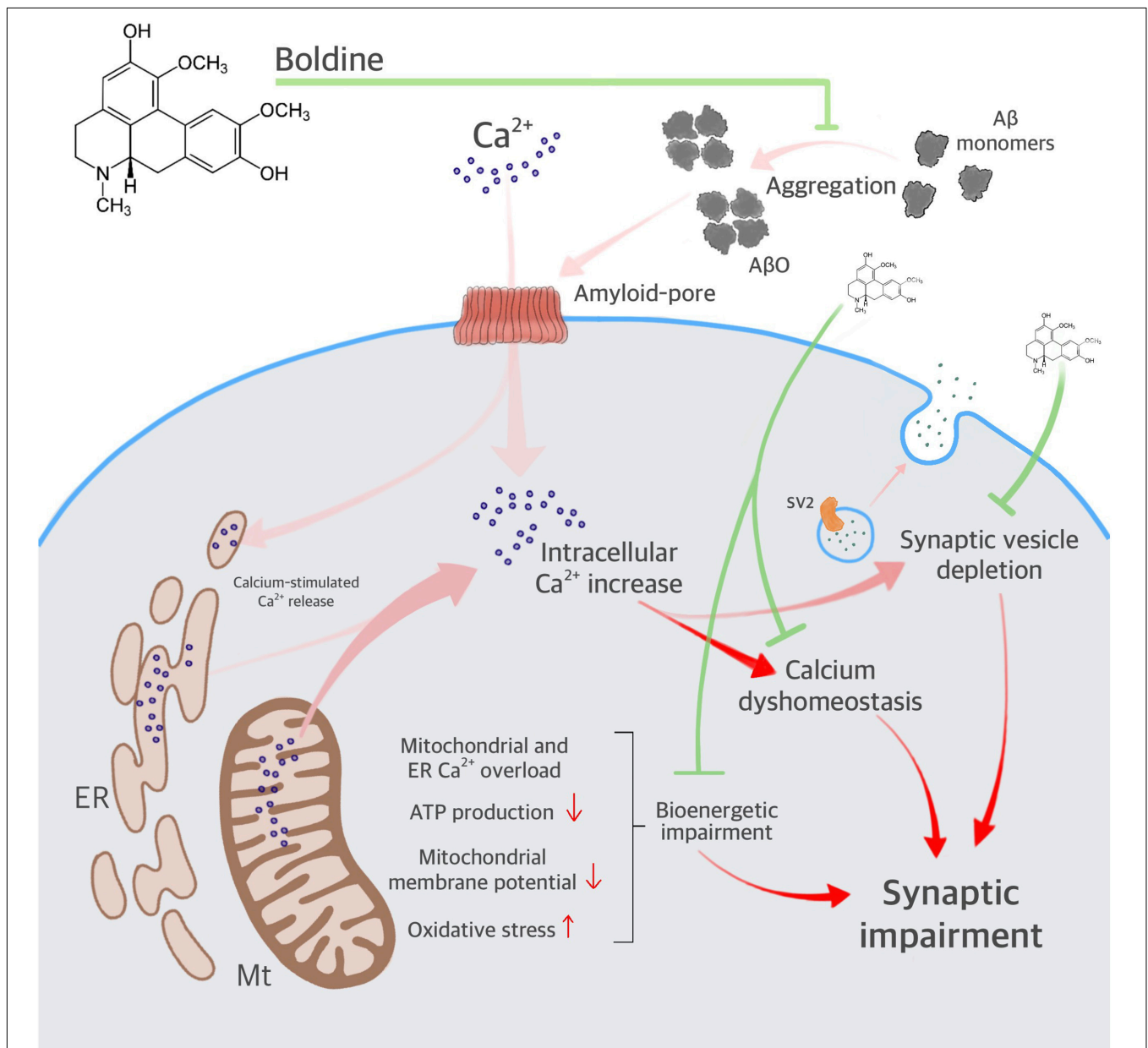


FIGURE 7 | Proposed mechanisms for boldine neuroprotection against A β O-induced synaptic failure and mitochondrial dysfunction. The scheme depicts A β O aggregation, increasing intracellular Ca^{2+} , and synaptic impairment. A β O also increases endoplasmic reticulum (ER) and mitochondrial (Mt) Ca^{2+} accumulation, contributing to calcium dyshomeostasis and bioenergetic impairment. Deregulation in intracellular Ca^{2+} leads to synaptic failure. Boldine interferes with the toxicity of A β O by inhibiting major steps in the amyloid cascade including membrane and organelle dyshomeostasis.

reported that boldine inhibited the opening of the mitochondrial membrane permeability transition pore (mPTP) that leads to an increase in ROS. Dhingra and Soni (2018) also found that boldine (6 mg/kg) reduced malondialdehyde (MDA) levels, a product of lipid peroxidation and an indicator of oxidative damage. This is in agreement with the well described antioxidant activity of boldine, which can react with free radicals due to its polyphenolic structure (Valenzuela et al., 1991).

Our data indicate that boldine interacts with the A β _{1–42} peptide, reduces A β O aggregation, and attenuates A β O-induced synaptic impairment (Figure 7). Furthermore, boldine restores A β O compromised mitochondrial function, including ER- and mitochondrial Ca²⁺ accumulation, disruption of $\Delta\Psi_m$, overproduction of mitochondrial ROS and mitochondrial respiration, namely maximal respiration, proton leak, and spare respiratory capacity in A β O-treated cells (unchanged OCR values when compared to the control). Therefore, the neuroprotective effect of boldine may result from: (1) Interaction with residues implicated in the association of A β to the membrane and the formation of channels permeable to Ca²⁺; (2) Interaction with residues implicated in ion permeation (mainly Ca²⁺) through the cellular membrane (i.e., histidines 13 and 14); (3) Direct interaction with A β , preventing ER and mitochondria deregulation due to Ca²⁺ rise, thus ameliorating mitochondrial function. In conclusion, low concentrations of boldine interfere with A β aggregation, prevent synaptic failure and organelle dysfunction, centering on mitochondria as one of the relevant players relevant for cell survival, and thus constituting a potential neuroprotective drug in AD.

DATA AVAILABILITY STATEMENT

The raw data supporting the conclusions of this article will be made available by the authors, without undue reservation.

REFERENCES

- Aguayo, L. G., and Pancetti, F. C. (1994). Ethanol modulation of the gamma-aminobutyric acidA- and glycine-activated Cl- current in cultured mouse neurons. *J. Pharmacol. Exp. Ther.* 270, 61–69.
- Arispe, N. (2004). Architecture of the Alzheimer's A beta P ion channel pore. *J. Membr. Biol.* 197, 33–48. doi: 10.1007/s00232-003-0638-7
- Arispe, N., Diaz, J. C., and Flora, M. (2008). Efficiency of histidine-associating compounds for blocking the Alzheimer's A β channel activity and cytotoxicity. *Biophys. J.* 95, 4879–4889. doi: 10.1529/biophysj.108.135517
- Backhouse, N., Delporte, C., Givernau, M., Cassels, B. K., Valenzuela, A., and Speisky, H. (1994). Anti-inflammatory and antipyretic effects of boldine. *Agents Actions* 42, 114–117. doi: 10.1007/BF01983475
- Bannach, R., Valenzuela, A., Cassels, B. K., Núñez-Vergara, L. J., and Speisky, H. (1996). Cytoprotective and antioxidant effects of boldine on tert-butyl hydroperoxide-induced damage to isolated hepatocytes. *Cell Biol. Toxicol.* 12, 89–100. doi: 10.1007/BF00143359
- Beck, S. J., Guo, L., Phensy, A., Tian, J., Wang, L., Tandon, N., et al. (2016). Deregulation of mitochondrial F1FO-ATP synthase via OSCP in Alzheimer's disease. *Nat. Commun.* 7:11483. doi: 10.1038/ncomms11483
- Ben-Hail, D., Begas-Shvartz, R., Shalev, M., Shteiinfer-Kuzmine, A., Gruzman, A., Reina, S., et al. (2016). Novel compounds targeting the mitochondrial protein VDAC1 inhibit apoptosis and protect against mitochondrial dysfunction. *J. Biol. Chem.* 291, 24986–25003. doi: 10.1074/jbc.M116.744284
- Cassels, B. K., Fuentes-Barros, G., and Castro-Saavedra, S. (2018). Boldo, its secondary metabolites and their derivatives. *Curr. Tradit. Med.* 5, 31–65. doi: 10.2174/2215083804666181113112928
- Cline, E. N., Bicca, M. A., Viola, K. L., and Klein, W. L. (2018). The amyloid- β oligomer hypothesis: beginning of the third decade. *J. Alzheimers Dis.* 64(Suppl. 1), S567–S610. doi: 10.3233/JAD-179941
- Csordás, G., Weaver, D., and Hajnóczky, G. (2018). Endoplasmic reticulum–mitochondrial contactology: structure and signaling functions. *Trends Cell Biol.* 28, 523–540. doi: 10.1016/j.tcb.2018.02.009
- Cummings, J., Lee, G., Ritter, A., Sabbagh, M., and Zhong, K. (2019). Alzheimer's disease drug development pipeline: 2019. *Alzheimers Dement. Transl. Res. Clin. Interv.* 5, 272–293. doi: 10.1016/j.trci.2019.05.008
- Davis, J. B., and Maher, P. (1994). Protein kinase C activation inhibits glutamate-induced cytotoxicity in a neuronal cell line. *Brain Res.* 652, 169–173. doi: 10.1016/0006-8993(94)90334-4
- De Felice, F. G., Wu, D., Lambert, M. P., Fernandez, S. J., Velasco, P. T., Lacor, P. N., et al. (2008). Alzheimer's disease-type neuronal tau hyperphosphorylation induced by A β oligomers. *Neurobiol. Aging.* 29, 1334–1347. doi: 10.1016/j.neurobiolaging.2007.02.029

ETHICS STATEMENT

The animal study was reviewed and approved by the Ethics Committee at the University of Concepcion.

AUTHOR CONTRIBUTIONS

JT, EF-P, IF, ACR, and LA wrote the manuscript, designed *in vitro* experiments, and discussed the results. CB designed and performed *in silico* studies and analysis. JT, EF-P, NR-L, BP-C, LP-P, and DM carried out material preparation, data collection and analysis of *in vitro* studies. All authors read and approved the final manuscript.

FUNDING

This work was supported by FONDECYT 1180752 (LA). This work was financed by the European Regional Development Fund (ERDF), through the Centro 2020 Regional Operational Programme under project CENTRO-01-0145-FEDER-000012-HealthyAging2020 (ACR) and through the COMPETE 2020-Operational Programme for Competitiveness and Internationalisation and Portuguese national funds via FCT–“Fundação para a Ciência e a Tecnologia,” under projects POCI-01-0145-FEDER-032316 (IF, ACR) and UIDB/04539/2020, and FCT fellowship ref: FCT 2020.07951.BD.

ACKNOWLEDGMENTS

We would like to thank Lauren Aguayo for having read and provided useful suggestions to the manuscript. For technical support we thank Lauren Aguayo, Carolina Benitez, Ixia Cid and Jocelin González.

- De Lima, N. M. R., Ferreira, E. D. O., Fernandes, M. Y. S. D., Lima, F. A. V., Neves, K. R. T., Do Carmo, M. R. S., et al. (2016). Neuroinflammatory response to experimental stroke is inhibited by boldine. *Behav. Pharmacol.* 28, 223–237. doi: 10.1097/FBP.0000000000000265
- Dhingra, D., and Soni, K. (2018). Behavioral and biochemical evidences for nootropic activity of boldine in young and aged mice. *Biomed. Pharmacother.* 97, 895–904. doi: 10.1016/j.biopha.2017.11.011
- Ferreira, I. L., Bajouco, L. M., Mota, S. I., Auberson, Y. P., Oliveira, C. R., and Rego, A. C. (2012a). Amyloid beta peptide 1–42 disturbs intracellular calcium homeostasis through activation of GluN2B-containing N-methyl-d-aspartate receptors in cortical cultures. *Cell Calcium* 51, 95–106. doi: 10.1016/j.ceca.2011.11.008
- Ferreira, I. L., Carmo, C., Naia, L. I., Mota, S., and Cristina Rego, A. (2018). Assessing mitochondrial function in in vitro and ex vivo models of Huntington's disease. *Methods Mol. Biol.* 8, 415–442. doi: 10.1007/978-1-4939-7825-0_19
- Ferreira, I. L., Ferreiro, E., Schmidt, J., Cardoso, J. M., Pereira, C. M. F., Carvalho, A. L., et al. (2015). A β and NMDAR activation cause mitochondrial dysfunction involving ER calcium release. *Neurobiol. Aging* 36, 680–692. doi: 10.1016/j.neurobiolaging.2014.09.006
- Ferreira, I. L., Resende, R., Ferreiro, E., Rego, A. C., and Pereira, C. F. (2012b). Multiple defects in energy metabolism in Alzheimers disease. *Curr. Drug Targets* 11, 1193–1206. doi: 10.2174/1389450111007011193
- Ferreira, E., Baldeiras, I., Ferreira, I. L., Costa, R. O., Rego, A. C., Pereira, C. F., et al. (2012). Mitochondrial- and endoplasmic reticulum-associated oxidative stress in alzheimers disease: From pathogenesis to biomarkers. *Int. J. Cell Biol.* 2012:735206. doi: 10.1155/2012/735206
- Gómez, G. I., and Velarde, V. (2018). Boldine improves kidney damage in the goldblatt 2K1C model avoiding the increase in TGF- β . *Int. J. Mol. Sci.* 19:1864. doi: 10.3390/ijms19071864
- González-Sanmiguel, J., Burgos, C. F., Bascuñán, D., Fernández-Pérez, E. J., Riffollepe, N., Boopathi, S., et al. (2020). Gabapentin inhibits multiple steps in the amyloid beta toxicity cascade. *ACS Chem. Neurosci.* 19, 3064–3076. doi: 10.1021/acscchemneuro.0c00414
- Hanaki, M., Murakami, K., Katayama, S., Akagi, K., Akagi, K. I., and Irie, K. (2018). Mechanistic analyses of the suppression of amyloid β 42 aggregation by apomorphine. *Bioorganic Med. Chem.* 26, 1538–1546. doi: 10.1016/j.bmc.2018.01.028
- Heidari, R., Arabnezhad, M. R., Ommati, M. M., Azarpira, N., Ghodsimanesh, E., and Niknahad, H. (2019). Boldine supplementation regulates mitochondrial function and oxidative stress in a rat model of hepatotoxicity. *Pharm. Sci.* 25, 1–10. doi: 10.15171/PS.2019.1
- Hernández-Salinas, R., Vielma, A. Z., Arismendi, M. N., Boric, M. P., Sáez, J. C., and Velarde, V. (2013). Boldine prevents renal alterations in diabetic rats. *J. Diabetes Res.* 2013:593672. doi: 10.1155/2013/593672
- Himeno, E., Ohyagi, Y., Ma, L., Nakamura, N., Miyoshi, K., Sakae, N., et al. (2011). Apomorphine treatment in Alzheimer mice promoting amyloid- β degradation. *Ann. Neurol.* 69, 248–256. doi: 10.1002/ana.22319
- Jang, Y. Y., Song, J. H., Shin, Y. K., Han, E. S., and Lee, C. S. (2000). Protective effect of boldine on oxidative mitochondrial damage in streptozotocin-induced diabetic rats. *Pharmacol. Res.* 42, 361–371. doi: 10.1006/phrs.2000.0705
- Jarrett, J. T., and Lansbury, P. T. (1993). Seeding "one-dimensional crystallization" of amyloid: a pathogenic mechanism in Alzheimer's disease and scrapie? *Cell* 73, 1055–1058. doi: 10.1016/0092-8674(93)90635-4
- Kim, W., and Hecht, M. H. (2006). Generic hydrophobic residues are sufficient to promote aggregation of the Alzheimer's A β 42 peptide. *Proc. Natl. Acad. Sci. U.S.A.* 103, 15824–15829. doi: 10.1073/pnas.0605629103
- Konrath, E. L., Santin, K., Nassif, M., Latini, A., Henriques, A., and Salbego, C. (2008). Antioxidant and pro-oxidant properties of boldine on hippocampal slices exposed to oxygen-glucose deprivation in vitro. *Neurotoxicology* 29, 1136–1140. doi: 10.1016/j.neuro.2008.05.008
- Lambert, M. P., Barlow, A. K., Chromy, B. A., Edwards, C., Liosatos, M. F., Morgan, T. E., et al. (1998). Diffusible, nonfibrillar ligands derived from A β 1-42 are potent central nervous system neurotoxins. *Proc. Natl. Acad. Sci. U.S.A.* 95, 6448–6453.
- Lau, Y. S., Tian, X. Y., Mustafa, M. R., Murugan, D., Liu, J., Zhang, Y., et al. (2013). Boldine improves endothelial function in diabetic db/db mice through inhibition of angiotensin II-mediated BMP4-oxidative stress cascade. *Br. J. Pharmacol.* 170, 1190–1198. doi: 10.1111/bph.12350
- Lei, M., Xu, H., Li, Z., Wang, Z., O'Malley, T. T., Zhang, D., et al. (2016). Soluble A β oligomers impair hippocampal LTP by disrupting glutamatergic/GABAergic balance. *Neurobiol. Dis.* 85, 111–121. doi: 10.1016/j.nbd.2015.10.019
- Lin, W. H., Ciccotosto, G. D., Giannakis, E., Tew, D. J., Perez, K., Masters, C. L., et al. (2008). Amyloid- β peptide (A β) neurotoxicity is modulated by the rate of peptide aggregation: A β dimers and trimers correlate with neurotoxicity. *J. Neurosci.* 28, 11950–11958. doi: 10.1523/JNEUROSCI.3916-08.2008
- Masters, C. L., Bateman, R., Blennow, K., Rowe, C. C., Sperling, R. A., and Cummings, J. L. (2015). Alzheimer's disease. *Nat. Rev. Dis. Prim.* 1:15056. doi: 10.1038/nrdp.2015.56
- Moezi, L., Yahosseini, S., Jamshidzadeh, A., Dastgheib, M., and Pirsalami, F. (2018). Sub-chronic boldine treatment exerts anticonvulsant effects in mice. *Neurol. Res.* 40, 146–152. doi: 10.1080/01616412.2017.1402500
- Mota, S. I., Costa, R. O., Ferreira, I. L., Santana, I., Caldeira, G. L., Padovano, C., et al. (2015). Oxidative stress involving changes in Nrf2 and ER stress in early stages of Alzheimer's disease. *Biochim. Biophys. Acta Mol. Basis Dis.* 1852, 1428–1441. doi: 10.1016/j.bbdis.2015.03.015
- Naia, L., Ferreira, I. L., Ferreiro, E., and Rego, A. C. (2017). Mitochondrial Ca $^{2+}$ handling in Huntington's and Alzheimer's diseases – Role of ER-mitochondria crosstalk. *Biochem. Biophys. Res. Commun.* 483, 1069–1077. doi: 10.1016/j.bbrc.2016.07.122
- Nakamura, M., Shishido, N., Nunomura, A., Smith, M. A., Perry, G., Hayashi, Y., et al. (2007). Three histidine residues of amyloid- β peptide control the redox activity of copper and iron. *Biochemistry* 46, 12737–12743. doi: 10.1021/bi701079z
- Parodi, J., Sepúlveda, F. J., Roa, J., Opazo, C., Inestrosa, N. C., and Aguayo, L. G. (2010). Beta-amyloid causes depletion of synaptic vesicles leading to neurotransmission failure. *J. Biol. Chem.* 285, 2506–2514. doi: 10.1074/jbc.M109.030023
- Peters, C., Bascuñán, D., Burgos, C. F., Bobadilla, C., González-Sanmiguel, J., Boopathi, S., et al. (2020). Characterization of a new molecule capable of inhibiting several steps of the amyloid cascade in Alzheimer's disease. *Neurobiol. Dis.* 141:104938. doi: 10.1016/j.nbd.2020.104938
- Peters, C., Fernandez-Perez, E. J., Burgos, C. F., Espinoza, M. P., Castillo, C., Urrutia, J. C., et al. (2013). Inhibition of amyloid beta-induced synaptotoxicity by a pentapeptide derived from the glycine zipper region of the neurotoxic peptide. *Neurobiol. Aging* 34:1. doi: 10.1016/j.neurobiolaging.2013.06.001
- Reddy, P. H., and Beal, M. F. (2008). Amyloid beta, mitochondrial dysfunction and synaptic damage: implications for cognitive decline in aging and Alzheimer's disease. *Trends Mol. Med.* 14, 45–53. doi: 10.1016/j.molmed.2007.12.002
- Resende, R., Ferreiro, E., Pereira, C., and Resende de Oliveira, C. (2008). Neurotoxic effect of oligomeric and fibrillar species of amyloid-beta peptide 1–42: Involvement of endoplasmic reticulum calcium release in oligomer-induced cell death. *Neuroscience* 155, 725–737. doi: 10.1016/j.neuroscience.2008.06.036
- Rhein, V., Song, X., Wiesner, A., Ittner, L. M., Baysang, G., Meier, F., et al. (2009). Amyloid- β and tau synergistically impair the oxidative phosphorylation system in triple transgenic Alzheimer's disease mice. *Proc. Natl. Acad. Sci. U.S.A.* 106, 20057–20062. doi: 10.1073/pnas.0905529106
- Sage, D., Donati, L., Soulez, F., Fortun, D., Schmit, G., Seitz, A., et al. (2017). DeconvolutionLab2: an open-source software for deconvolution microscopy. *Methods, Elsevier* 115, 28–41. doi: 10.1016/j.ymeth.2016.12.015
- Sepúlveda, F. J., Fierro, H., Fernandez, E., Castillo, C., Peoples, R. W., Opazo, C., et al. (2014). Nature of the neurotoxic membrane actions of amyloid- β on hippocampal neurons in Alzheimer's disease. *Neurobiol. Aging* 35, 472–481. doi: 10.1016/j.neurobiolaging.2013.08.035
- Shankar, G. M., Bloodgood, B. L., Townsend, M., Walsh, D. M., Selkoe, D. J., and Sabatini, B. L. (2007). Natural oligomers of the Alzheimer amyloid-beta protein induce reversible synapse loss by modulating an NMDA-type glutamate receptor-dependent signaling pathway. *J. Neurosci.* 27, 2866–2875. doi: 10.1523/JNEUROSCI.4970-06.2007
- Smilansky, A., Dangoor, L., Nakdimon, I., Ben-Hail, D., Mizrachi, D., and Shoshan-Barmatz, V. (2015). The voltage-dependent anion channel 1 mediates amyloid β toxicity and represents a potential target for Alzheimer disease therapy. *J. Biol. Chem.* 290, 30670–30683. doi: 10.1074/jbc.M115.691493

- Snyder, E. M., Nong, Y., Almeida, C. G., Paul, S., Moran, T., Choi, E. Y., et al. (2005). Regulation of NMDA receptor trafficking by amyloid- β . *Nat. Neurosci.* 8, 1051–1058. doi: 10.1038/nn1503
- Terry, R. D., Masliah, E., Salmon, D. P., Butters, N., DeTeresa, R., Hill, R., et al. (1991). Physical basis of cognitive alterations in alzheimer's disease: synapse loss is the major correlate of cognitive impairment. *Ann. Neurol.* 30, 572–580. doi: 10.1002/ana.410300410
- Tewari, D., Stankiewicz, A. M., Mocan, A., Sah, A. N., Tzvetkov, N. T., Huminiecki, L., et al. (2018). Ethnopharmacological approaches for dementia therapy and significance of natural products and herbal drugs. *Front. Aging Neurosci.* 10:3. doi: 10.3389/fnagi.2018.00003
- Valenzuela, A., Nieto, S., Cassels, B. K., and Speisky, H. (1991). Inhibitory effect of boldine on fish oil oxidation. *J. Am. Oil Chem. Soc.* 68, 935–937. doi: 10.1007/BF02657538
- Weidner, W. S., and Barbarino, P. (2019). P4-443: the state of the art of dementia research: new frontiers. *Alzheimers Dement* 15, 1473–1473. doi: 10.1016/j.jalz.2019.06.4115
- Yi, C., Ezan, P., Fernández, P., Schmitt, J., Sáez, J. C., Giaume, C., et al. (2017). Inhibition of glial hemichannels by boldine treatment reduces neuronal suffering in a murine model of Alzheimer's disease. *Glia* 65, 1607–1625. doi: 10.1002/glia.23182
- Youn, Y. C., Kwon, O. S., Han, E. S., Song, J. H., Shin, Y. K., and Lee, C. S. (2002). Protective effect of boldine on dopamine-induced membrane permeability transition in brain mitochondria and viability loss in PC12 cells. *Biochem. Pharmacol.* 63, 495–505. doi: 10.1016/S0006-2952(01)00852-8

Conflict of Interest: The authors declare that the research was conducted in the absence of any commercial or financial relationships that could be construed as a potential conflict of interest.

Copyright © 2021 Toledo, Fernández-Pérez, Ferreira, Marinho, Riffo-Lepe, Pineda-Cuevas, Pinochet-Pino, Burgos, Rego and Aguayo. This is an open-access article distributed under the terms of the Creative Commons Attribution License (CC BY). The use, distribution or reproduction in other forums is permitted, provided the original author(s) and the copyright owner(s) are credited and that the original publication in this journal is cited, in accordance with accepted academic practice. No use, distribution or reproduction is permitted which does not comply with these terms.